Support vector machine (SVM) based liver classification: fibrosis, steatosis, and inflammation

Jihye Baek
Department of Electrical and Comupter Engineering
University of Rochester
Rochester, NY, USA
jbaek7@ur.rochester.edu

Terri A. Swanson
Pfizer Inc.
Cambridge, MA, USA
terri.a.swanson@pfizer.com

Theresa Tuthill
Pfizer Inc.
Cambridge, MA, USA
theresa.tuthill@pfizer.com

Kevin J. Parker
Department of Electrical and Comupter Engineering
University of Rochester
Rochester, NY, USA
kevin.parker@rochester.edu

***Abstract*— An SVM based liver classifier was developed to differentiate liver conditions, including normal, fibrosis with low fat, fibrosis with high fat, and inflammation.**

An in-vivo study was performed with 35 rats under normal conditions or after carbon tetrachloride (CCl_4) or concanavalin A (ConA) dosing to induce fibrosis with varying degrees of steatosis, and inflammation, respectively. These livers were imaged in-vivo by an ultrasound, and approximately 30 frames for each rat were acquired. Therefore, a total of 998 ultrasound images were analyzed and used for training a SVM classifier. Each image has three measured parameters: H-scan scattering classification, estimated attenuation coefficient, and B-scan intensity. These parameters were assigned as inputs to the SVM.

A liver diagnosis system based on the SVM and H-scan was produced. The clusters representing each state of liver are provided in two- and three- parameter space. From these, the SVM generates decision planes to classify the liver conditions. The classification accuracy is 92.2% with the three features. Therefore, these results provide the beginning of a coherent framework for determining the scattering signatures or clustering in multi-parametric space, of the normal liver compared with diseased livers.

Keywords— ultrasound scatter, liver classification, support vector machine, multiparametric analysis

I. Introduction

A longstanding priority within diagnostic imaging is the assessment of the structural and functional condition of the liver (Taylor and Ros 1998; Ozturk et al. 2018). Ultrasound scanners have been commonly used for screening and diagnosing livers due to their advantages in providing non-invasive, portable, inexpensive medical imaging. Therefore, previous research to quantify measurements from ultrasound liver scans and to classify liver conditions from ultrasound-related parameters have shown promise (Chivers and Hill 1975; Bamber 1979; Campbell and Waag 1984; Zagzebski et al. 1993; Higuchi et al. 2014; Al-Kadi et al. 2016; Liao et al. 2016; Zhou et al. 2018; Lin et al. 2019). In addition, some multiparametric clusters were assessed (Momenan *et al.*, 1987; Momenan *et al.*, 1994). Recent characterization studies using ultrasound have employed machine learning tools (Virmani *et al.*, 2013; Singh *et al.*, 2014; Byra *et al.*, 2018; Andrade *et al.*, 2012; Wu et al. 2012). However, those rely on the log-compressed B-scan images that contains less signal than radiofrequency (RF) data and depend on machine settings and users. Thus, this study estimated parameters using RF data and formed clusters related to liver pathology in a multi-dimensional space. Subsequently, an SVM analysis resulted in decision planes which can be used to categorize pathological liver states, including fibrosis, steatosis, and inflammation.

This work first measured three parameters from the H-scan analysis, related to scattering and attenuation estimations, and B-scan intensity. Secondly, we implemented the SVM classifier within the four classes confirmed by pathology: normal, fibrosis with low fat, fibrosis with high fat, and inflammation. Finally, the decision planes of the SVM were shown in multi-parametric spaces with the clusters of liver conditions, producing high accuracy in discriminating between groups.

II. Methods

A. Study design and Data acquisition

An in-vivo study was performed and all experimental protocols were approved by the Pfizer Animal Care and Use Committee (IACUC). A total of 35 rats were enrolled, 4 TAC NIH: rnu (nude, Taconic Biosciences, Inc., Rensselaer, NY, USA) and 31 Sprague-Dawley rats (SD, Charles River Laboratories, Wilmington, MA, USA). We investigated the rat under normal conditions and after inducing liver disease, by using CCl_4 or ConA exposure. These caused a fibrotic response with varying degrees of fat accumulation, or inflammation, as confirmed by post-mortem pathology of Trichrome stain, Picro-Sirius red, and Oil Red O stain. It resulted in 4 groups: 9 rats for normal, 6 for fibrosis with high

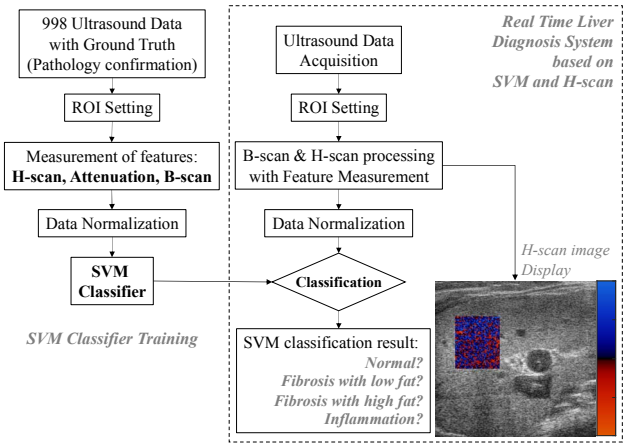

Figure 1. Design of the proposed liver classification system based on H-scan and SVM

978-1-7281-5448-0/20/$31.00 ©2020 IEEE

fat (> 9%), 11 for fibrosis with low fat (< 6.5%), and 9 for inflammation.

Ultrasound scans were performed at 8 weeks after starting the protocol. A Vevo 2100 (Visual Sonics, Toronto, Canada) scanner with a 21 MHz center frequency linear transducer (MS 250) acquired RF data under the consistent scan settings, including the gain, and focal depth, etc. Every scan has approximately 30 frames, and therefore the total of 998 ultrasound images were obtained for the SVM processing. Each image has three measured features from H-scan classification, estimated attenuation coefficient, and B-scan intensity. These parameters were assigned as inputs to train a SVM classifier.

This study aims to construct a liver classifier based on SVM and H-scan, which can be a real-time diagnosing system, as shown in **Figure 1**. While scanning a liver, a rectangular ROI is set by user, similar to the use of color doppler imaging. The system processes B-scan and H-scan and measures the three features within the ROI. Then, the SVM classifier outputs the estimated liver condition, and a H-scan image is displayed. This study designed the overall approach, and then built the trained SVM classifier and H-scan processor.

B. Feature Measurement: H-scan, Attenuation, and B-scan

As a matched filter analysis to classify scattering signatures of tissues, H-scan method was developed (Parker 2016; Parker and Baek, 2020; Baek *et al.*, 2020; Baek *et al.*, in press) to analyze the power law transfer functions in frequency domain of ultrasound signal. The received RF signal $r(t)$ containing scattering signatures is interpreted by convolution with a bandpass filter related to the Gaussian family and described by:

$$\max_{n}\left(r(t) * \mathcal{F}^{-1}(G_n(f))\right) \tag{1}$$

where $G_n(f)$ is the n-th Gaussian filter in frequency domain. The chosen n that maximizes the equation (1) has a corresponding Gaussian function with a peak frequency, which becomes the estimated peak frequency at the time point t. This study employed 256 color levels for the 256 filters, and therefore the estimated frequencies are mapped into a color ranging from red to blue; the color map is shown in **Figure 1**. However, the accumulated attenuation along with ultrasound propagation causes frequency shifts over depth, producing a gradual H-scan color bias from more blue to red. This attenuation accumulation was estimated by modeling the loss as $e^{-\alpha f x}$ where α is the attenuation coefficient in Np/MHz/cm, and f (MHz) is the estimated frequency at depth x (cm). Then, the attenuation coefficient can be derived:

$$\hat{\alpha} = -\frac{f - f_0}{x \cdot \sigma^2} \tag{2}$$

where f_0 and σ are a center frequency and bandwidth of a Gaussian function that models ultrasound transmission pulse, and f is estimated by H-scan; more details for estimation can be found in Baek *et al.*, 2020a; Baek *et al.*, 2020b *inpress*. Using the estimated coefficient, attenuation correction was performed; more details for correction can be found in Parker and Baek, 2020.

Therefore, this study produced three parameters: % of blue from H-scan representing a shift in scattering transfer function from the tissue, the attenuation coefficient (converted to units of dB/MHz/cm), and the intensity (dB) from B-scan. The % of blue is defined by;

$$\%\ of\ blue = \frac{n_B}{n_B + n_R} \tag{3}$$

where n_B and n_R are the number of blue and red pixels, which have color levels of [1, 128] and [129, 256], respectively. The attenuation coefficient was measured by the equation (2), and the dB scale intensity of log-compressed data from B-scan was measured from liver ROIs at constant depth.

The three parameters were used as the input features to the SVM after feature scaling to normalize the different scales of each feature. The feature scaling was performed by a modified min-max normalization:

$$x_{scale} = \frac{x - average(x_{NOR})}{\frac{1.0}{0.9} max(|\max(x) - average(x_{NOR})|, |\min(x) - average(x_{NOR})|)} \tag{4}$$

where $average(x_{NOR})$ is average value of normal data set.

C. The Support Vector Machine Classifier

To classify the liver conditions, the SVM classifier was implemented in MATLAB (The Mathworks, Inc., Natick, MA, USA). SVM classifiers were designed (Vapnik, 1999; Bishop, 2006; Cortes and Vapnik, 1995) to maximize the margins between classes and minimize penalties for misclassified vectors, which can be described by:

$$\min\left(\frac{1}{2}\|\vec{w}\|^2 + C\sum_{n=1}^{N}\xi_n\right) \tag{5}$$

where the first term relates to one over margin distance, and the second term represents the summation of penalties. C is a box constant to be optimized for the SVM classifier, and n denotes the support vectors near class boundaries. The solution of equation (5) is obtained by solving Lagrangian of the problem with a gaussian kernel function that has a parameter σ. For the parameters of C and σ, parameter optimization was performed based on the hyperplane shapes and classification accuracy by preventing under- or over-fitting; more details for the optimization can be found in Baek et al. 2020b. The classification accuracy is defined by:

$$Accuracy\ [\%] = \frac{Correctly\ classified\ \#}{Total\ \#\ of\ input\ data} \times 100\ \% \tag{6}$$

III. RESULTS

A. Feature measurements: H-scan, Attenuation, and B-scan

Figure 2(a) shows the measured raw data with different scales for each feature. The normalized data are in **Figure 2(b)**, of each feature has distribution between -1 and 1, showing the zero-mean of normal data and relative data

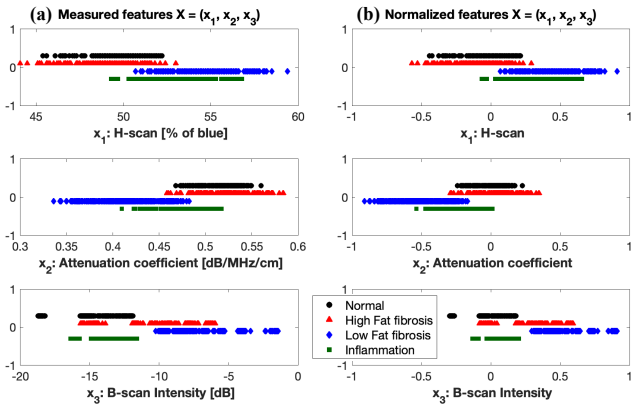

Figure 2. (a) Measured and (b) normalized features from H-scan, attenuation coefficient, and B-scan

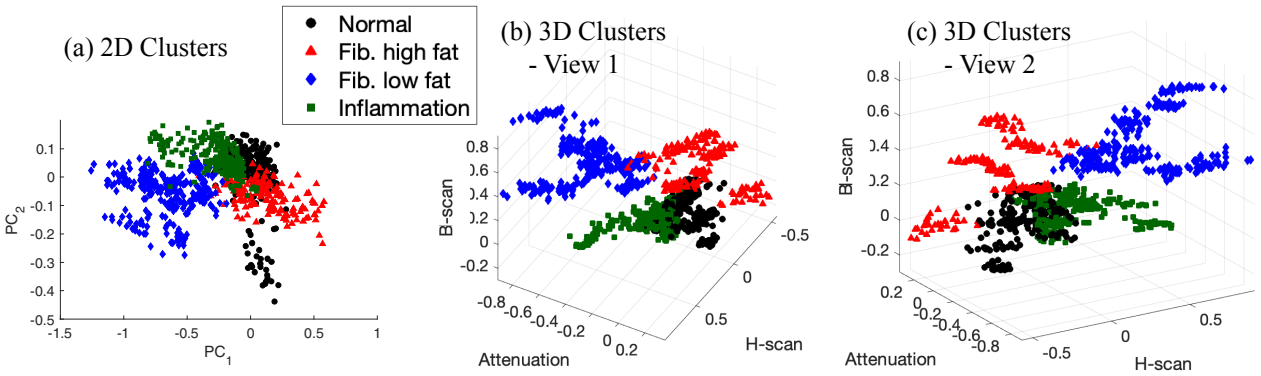

Figure 3. (a) 2D and (b) 3D view of clusters: normal, low fat fibrosis, high fat fibrosis, and inflammation.

positions of diseased cases compared to normals. Although no single parameter can differentiate among the 4 classes without overlap, each feature tends to discriminate specific groups. The H-scan provides the best separation between normal and inflammation, and attenuation estimation is also likely to distinguish inflammation from normal. The B-scan intensity separates fibrosis from the others. For the separation between normal and low fatty group, all the three measurements provide discrimination. The H-scan and attenuation tend to differentiate low and high fatty groups. The B-scan can separate low fatty fibrosis and inflammation. Multi-parametric analysis combines all these results for an improved classification.

Figure 3 (a) and (b) represent two-dimensional (2D) and three-dimensional (3D) view of clusters, respectively. For 2D view, principal component analysis (PCA) reduced the three parameters into two, and the retained variances are 84.9%, 13.0%, and 2.1% for the first, second, and third principal components (PC), respectively. **Figure 3(a)** exclusively used the first two PCs with 97.9% of retained variances. Combining the three features in 2D space provides better separation between the four liver groups compared to each feature results in **Figure 2**, but there are still overlaps between the groups.

Figure 3 (b, c) illustrates two views of clusters in 3D space by using all the three measured features with normalized scales. The 3D views provide better separation between groups with less overlaps compared to one-dimensional (1D) and 2D feature spaces. These well-discriminated clusters have potential to construct robust hyperplanes by the SVM classifier when the features are used as inputs of the classifier.

B. The SVM Classification

The SVM machine with the 3D features was trained with optimized parameters of $C = 7$ and $\sigma = 0.2$. Additionally, another SVM classifier was constructed by using the 2D PCs to investigate the effect of feature numbers.

Figure 4 (a) shows hyperplanes in 2D space, and due to the overlaps between the liver groups the accuracy resulted in 84.9%. However, the SVM classifier with 3D input features has 92.2% of classification accuracy, and these hyperplanes are illustrated in **Figure 4 (b,c)**. Since the 3D clusters provide better discrimination than 2D clusters, the classification accuracy from the 3D features is higher than the 2D input although the information loss is only 2.1%. As shown in **Figure 4 (b,c)**, the hyperplanes can distinguish the 4 liver groups.

IV. Discussion

This study implemented a liver ultrasound classifier by employing the H-scan as a frequency-dependent analysis and the SVM to define multi-parametric clusters and boundaries between groups.

B-scan images have been traditionally used for liver diagnosis. However, as shown in **Figure 2**, B-scan intensity does not help the diagnosis of inflammation since the intensity are comparable to that of normal. Although B-scan demonstrates brighter intensities for fibrosis cases compared

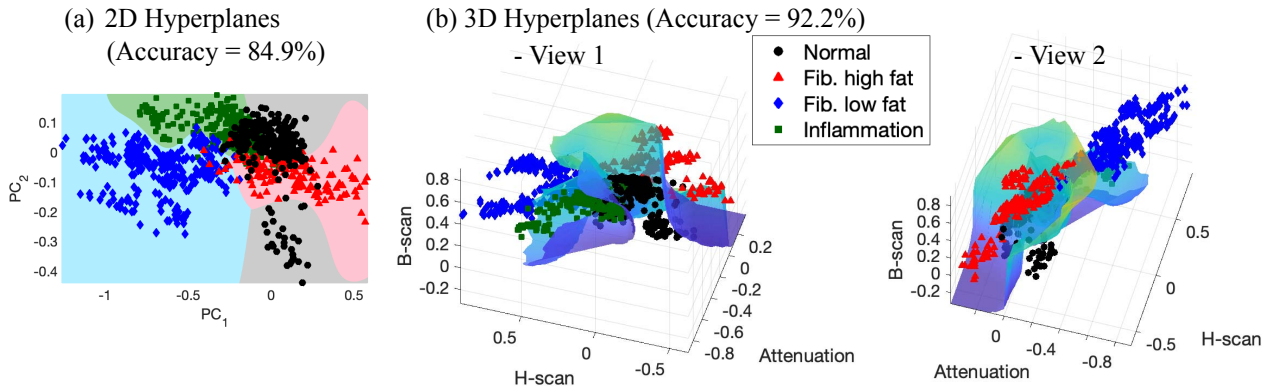

Figure 4. SVM results. (a) 2D hyperplanes with the first 2 principal components. (b) 3D hyperplanes with the 3 features.

to normals, it cannot differentiate the low and high fatty sub-groups within the fibrosis cases. To characterize liver conditions more accurately, the frequency-dependent investigations of H-scan and attenuation estimation were examined in this study, along with the echo-dependent approach of B-scan average intensity, or echogenicity. The two approaches can be considered independent, which thereby provides more complete. Therefore, the H-scan and attenuation estimates tend to discriminate the overlapped cases in B-scan: normal and inflammation; low and high fatty fibrosis. Consequently, utilizing all the three features offers the potential to discriminate the four liver with only minimal overlap between the conditions in multiparametric space.

In order to address the subtle overlaps for clear separation between the liver groups, a method that can combine the three data is required. Thus, this study employed the SVM as an effective way to classify the four conditions. The clusters of 3D space in **Figure 3** have better separation between groups than 1D feature space in **Figure 2**. Moreover, SVM provides a way to differentiate the liver conditions despite rare overlaps, providing smooth and robust hyperplanes while avoiding under- or over- fitting. The hyperplanes boundaries derived in this study can be used to classify new liver ultrasound scans.

By measuring the B-scan intensity, H-scan scattering frequency, and attenuation, this study demonstrated that the discrimination performance increased as more features were included; 2D clusters improve classification over any single parameter, and 3D parameters show more well separated clusters than 1D or 2D. Moreover, when the input features are more independent, they can offer more information within a joint analysis. For instance, echo- and frequency-based approaches resulted in different trends for discrimination, but H-scan and attenuation showed similar trends. Therefore, adding more parameters and parameters from different approaches can help to enhance the classification accuracy.

V. Conclusion

This study implemented the SVM classifier to improve liver diagnosis using the recently developed scattering analysis, the H-scan. This produces two output parameters, an H-scan scattering measurement and attenuation, and also provides color-coded images to visually assist the diagnosis. These parameters were sensitive to changes in liver conditions, which enable to construct clusters in multi-dimensional spaces, resulting in a robust SVM classification between the disease groups. This study verifies that H-scan measures based on biophysical models of scattering and wave propagation in liver tissues provide the ability to discriminate and classify pathological liver conditions.

Acknowledgment

This work was supported by National Institutes of Health grant R21EB025290 and by Pfizer Inc.

References

[1] Al-Kadi OS, Chung DYF, Coussios CC, Noble JA. Heterogeneous tissue characterization using ultrasound: a comparison of fractal analysis backscatter models on liver tumors. Ultrasound Med Biol 2016;42:1612-26.

[2] Andrade A, Silva J S, Santos J and Belo-Soares P 2012 Classifier approaches for liver steatosis using ultrasound images *Proc Technol* **5** 763-70

[3] Baek J, Ahmed R, Ye J, Gerber S A, Parker K J and Doyley M M 2020a H-scan, shear wave, and bioluminescent assessment of the progression of pancreatic cancer metastases in the liver, *in press Ultrasound Med Biol*

[4] Baek J, Poul S S, Swanson T A, Tuthill T and Parker K J 2020b Scattering signatures of normal vs. abnormal livers with support vector machine classification *in press Ultrasound Med Biol*

[5] Bamber JC. Theoretical modelling of the acoustic scattering structure of human liver. Acoust Lett 1979;3:114-9.

[6] Bishop CM. Pattern recognition and machine learning, Chapter 7. New York: Springer, pp. 325-358, 2006.

[7] Byra M, Styczynski G, Szmigielski C, Kalinowski P, Michałowski Ł, Paluszkiewicz R, Ziarkiewicz-Wróblewska B, Zieniewicz K, Sobieraj P and Nowicki A 2018 Transfer learning with deep convolutional neural network for liver steatosis assessment in ultrasound images *Int J Comput Assist Radiol Surg* **13** 1895-903

[8] Campbell JA, Waag RC. Measurements of calf liver ultrasonic differential and total scattering cross sections. J Acoust Soc Am 1984;75:603-11.

[9] Chivers RC, Hill CR. A spectral approach to ultrasonic scattering from human tissue: methods, objectives and backscattering measurements. Phys Med Biol 1975;20:799-815.

[10] Cortes C, Vapnik V. Support-vector networks. Mach Learn 1995;20:273-97.

[11] Higuchi T, Hirata S, Yamaguchi T, Hachiya H. Liver tissue characterization for each pixel in ultrasound image using multi-Rayleigh model. Jpn J Appl Phys 2014;53:07KF27.

[12] Liao YY, Yang KC, Lee MJ, Huang KC, Chen JD, Yeh CK. Multifeature analysis of an ultrasound quantitative diagnostic index for classifying nonalcoholic fatty liver disease. Sci Rep 2016;6:35083.

[13] Lin Y-H, Wan Y-L, Tai D-I, Tseng J-H, Wang C-Y, Tsai Y-W, Lin Y-R, Chang T-Y, Tsui P-H. Considerations of ultrasound scanning approaches in non-alcoholic fatty liver disease assessment through acoustic structure quantification. Ultrasound Med Biol 2019;45:1955-69.

[14] Momenan R, Insana M, Wagner R, Garra B and Loew M 1987 Application of cluster analysis and unsupervised learning to Multivariate tissue characterization vol 0768: SPIE

[15] Momenan R, Wagner R F, Garra B S, Loew M H and Insana M F 1994 Image staining and differential diagnosis of ultrasound scans based on the Mahalanobis distance *IEEE Trans Med Imaging* **13** 37-47

[16] Parker KJ. The H-scan format for classification of ultrasound scattering. J OMICS Radiol 2016;5:1000236.

[17] Parker KJ, Baek J. Fine-tuning the H-scan for discriminating changes in tissue scatterers. Biomed Phys Eng Express 2020;DOI: 10.1088/2057-1976/ab9206.

[18] Singh M, Singh S and Gupta S 2014 An information fusion based method for liver classification using texture analysis of ultrasound images *Inform Fusion* **19** 91-6

[19] Vapnik VN. An overview of statistical learning theory. IEEE Trans Neural Networks 1999;10:988-99.

[20] Virmani J, Kumar V, Kalra N, Khandelwal N. SVM-based characterization of liver ultrasound images using wavelet packet texture descriptors. J Digit Imaging 2013;26:530-43.

[21] Wu WJ, Lin SW, Moon WK. Combining support vector machine with genetic algorithm to classify ultrasound breast tumor images. Computerized medical imaging and graphics : the official journal of the Computerized Medical Imaging Society 2012;36:627-33.

[22] Zagzebski JA, Lu ZF, Yao LX. Quantitative ultrasound imaging: in vivo results in normal liver. Ultrason Imaging 1993;15:335-51.

[23] Zhou Z, Tai DI, Wan YL, Tseng JH, Lin YR, Wu S, Yang KC, Liao YY, Yeh CK, Tsui PH. Hepatic steatosis assessment with ultrasound small-window entropy imaging. Ultrasound Med Biol 2018;44:1327-40.